Temperature measurement of fragment emitting systems in Au+Au 35 MeV/nucleon collisions

P. M. Milazzo, G. Vannini, M. Azzano, D. Fontana, G. V. Margagliotti, P. F. Mastinu, R. Rui, and F. Tonetto
Dipartimento di Fisica and INFN, Trieste, Italy

N. Colonna
INFN, Bari, Italy

A. Botvina,* M. Bruno, M. D'Agostino, and M. L. Fiandri
Dipartimento di Fisica and INFN, Bologna, Italy

F. Gramegna
INFN, Laboratori Nazionali di Legnaro, Padova, Italy

I. Iori and A. Moroni
Dipartimento di Fisica and INFN, Milano, Italy

J. D. Dinius, S. Gaff, C. K. Gelbke, T. Glasmacher, M. J. Huang, G. J. Kunde, W. G. Lynch, L. Martin, C. P. Montoya, and H. Xi
Department of Physics and Astronomy and NSCL, Michigan State University, Michigan 48824
(Received 1 April 1998)

We report on the results of experiments performed to investigate the Au+Au 35 MeV/nucleon reaction. The reaction products generated in the disassembly of the unique source formed in central collisions and those coming from the decay of the quasiprojectile in peripheral and midperipheral ones (five different impact parameters) were identified through a careful data selection based on the study of energy and angular distributions. The excitation energies of the fragment sources have been extracted through a calorimetric method and by means of a comparison with model calculations. The nuclear temperatures of these decaying systems have been measured from the relative isotopic abundances and, also for central collisions, from the relative populations of excited states. The temperatures of the quasiprojectile disassembling systems are slowly increasing going towards smaller impact parameter. The relationship between temperature and excitation energy seems to be almost independent of the characteristics of the emitting source. The extracted caloric curve shows a slow monotonic increase with increasing excitation energy. A comparison with data derived from Au fragmentation at much higher incident energies is discussed. [S0556-2813(98)04408-2]

PACS number(s): 21.65.+f, 25.70.Pq, 64.30.+t

I. INTRODUCTION

Heavy-ion (HI) reactions at intermediate energies provide information on the general properties of nuclear matter in conditions very different from those of the ground state. The particular form of the nuclear forces leads, for infinite nuclear matter, to an equation of state (EOS) similar to that of the Van der Waals gas, which is likewise characterized by the existence of a liquid-gas phase transition [1]. For finite nuclear systems the situation is more complicated; however, several experiments [2] in HI reactions around the Fermi energy showed that many intermediate mass fragments (IMF) are produced with mass distributions following a power law behavior. Such a power law has been predicted for droplet condensation near the critical point in the liquid-gas phase diagram (droplet model of Fisher [3]). Moreover, microscopic statistical models predict the existence of a phase transition at excitation energies where nuclear systems undergo multifragment decays [4,5]. Results obtained in Au induced reactions by the Aladin, EOS, Miniball-MULTICS (M-M) Collaborations [6–9] seem to indicate the existence of signals related to a possible liquid-gas phase transition. While some of the results of EOS [7] and M-M Collaborations [9] suggest critical behaviors of some observables, the Aladin results [6] and other EOS data [8] rely on the measurement of the temperature of nuclear systems and on the particular shape of the caloric curve. The Aladin results [6] agree with predictions of statistical multifragmentation models [5] and are reminiscent of a (first order) phase transition while the EOS experiment [8] suggests that multifragmentation may result from a continuous phase transition near the critical point. The difference lies on the fact that there be [6] or not [8] a plateau of nearly constant temperature $T = 4.5-5.5$ MeV, for excitation energies ranging from about 4 to 10 MeV/nucleon. Moreover, measurements of the fragmentation of lighter projectiles (argon) at intermediate energies [10] display temperature values that increase monotonically and strongly with deduced excitation energy.

The M-M Collaboration in the Au+Au peripheral collisions at 35 MeV/nucleon found that the Z distribution of

*On leave from the Institute for Nuclear Research, 117312 Moscow, Russia.

fragments emitted by the quasiprojectile (QP) system in particular conditions follows a power law behavior [9] with an exponent of $\tau=2.2$ as expected by the Fisher model for a temperature near the critical one (T_c).

Here we present and discuss the results of temperature measurements of nuclear systems formed in central and in peripheral Au+Au collisions for different conditions of excitation energies, for an incident energy of 35 MeV/nucleon. A region of deduced excitation energy is investigated where the temperature was observed alternatively to be roughly constant or slowly increasing as a function of excitation energy in the case of Au fragmentation at much higher energies or to be monotonically and strongly increasing in the case of Argon fragmentation at intermediate energies.

The aim of this study is to investigate the caloric curve of finite nuclear matter, for systems having large size and definite characteristics of equilibration and decay, to study its incident energy dependence, and to get information on the existence or nonexistence of a quasi-plateau in the temperature-excitation energy relationship.

In Sec. II a brief description of the experimental conditions is given; Sec. III is devoted to describe the methods of temperature measurements and the prescriptions of emitting system identification. In Sec. IV the experimental results are presented and discussed, then the conclusions are drawn in Sec. V.

II. EXPERIMENTAL METHOD

In order to investigate the reaction Au+Au at 35 MeV/nucleon two experiments were performed at the National Superconducting K1200 Cyclotron Laboratory of the Michigan State University. Light charged particles and fragments with charge up to $Z=20$ were detected at $23°<\theta_{lab}<160°$ by the phoswich detectors of the MSU Miniball hodoscope [11]. The charge identification thresholds were about 2, 3, 4 MeV/nucleon in the Miniball for $Z=3,10,18$, respectively. The angular range $3°<\theta_{lab}<23°$ was covered by the MULTICS array [12]. The identification thresholds in the MULTICS array were about 1.5 MeV/nucleon for charge identification and about 10 MeV/nucleon for mass identification. The MULTICS array consisted of 48 telescopes, each of which was composed of an ionization chamber (IC), a silicon position-sensitive detector (Si) and a CsI crystal. Typical energy resolutions were 2%, 1%, and 5% for IC, Si and CsI, respectively. The geometric acceptance of the combined array was greater than 87% of 4π.

In a the two experiments, different gains were used for the MULTICS detectors; one experiment used low amplification gains (LAG experiment) to detect reaction products with charge up to $Z=83$, the other used higher amplification gains (HAG experiment) to allow good isotopic resolution from light particles up to carbon (Fig. 1). The multiplicity of detected charged particles (Nc) was used for impact parameter selection [13]:

$$\hat{b}=b/b_{max}=\left(\int_{Nc}^{+\infty}P(N'c)dN'c\right)^{1/2}.$$

Here $P(Nc)$ is the charged particle probability distribution and $\pi\cdot b_{max}^2$ is the measured reaction cross section for $Nc\geqslant 3$.

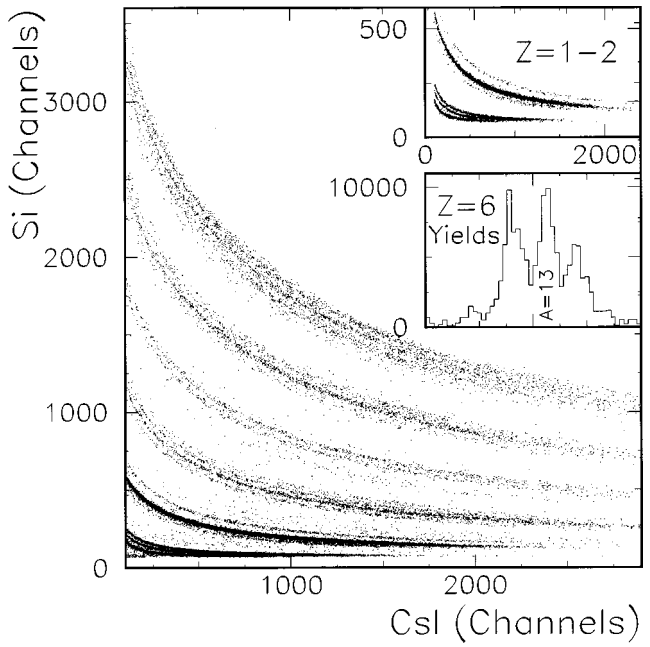

FIG. 1. Typical ΔE-E matrix for charge and mass identification. The isotope resolution is satisfactory from H to C. The inserts show the ΔE-E matrix for H and He isotopes (upper panel) and the particle identification function for $Z=6$ (lower panel).

To obtain the matching between the two experiments we used the Miniball as a counter to make comparison via Nc multiplicities.

III. CHARACTERIZATION OF THE FRAGMENT EMISSION SOURCE AND MEASUREMENTS OF ITS TEMPERATURE

To gain more insight into the characteristics of the caloric curve of finite nuclear systems and the possible existence of a phase transition, one must measure the temperatures of well defined and experimentally identified systems, of different excitation energy and size, using reliable thermometers.

In HI reactions at intermediate energies several different decaying systems are formed depending on impact parameter. These systems emit fragments (light, intermediate and heavy mass fragments), i.e., they behave as fragment sources which differ in size, shape, excitation energy, and even the way in which they are formed. For central collisions of symmetric systems at $E/A\geqslant 50$ MeV, collective motion effects [14], such as the radial flow, must be taken into account. Such collective motion affects the mechanism of fragment formation and decreases the available thermal energy of the fused system. When experimental results from different reactions, at different impact parameters and different incident energies, are used to construct a caloric curve, particular care must be taken in drawing conclusions. The Au+Au reaction at 35 MeV/nucleon is well suited for an investigation of the nuclear caloric curve, because the nuclear systems formed in central, midperipheral, and peripheral, collisions are relatively large in size (the smallest piece of nuclear matter has the size of the order of a Au nucleus) and thus apt for thermodynamical treatments. Moreover, the incident energy is sufficiently low to render collective expansion unimportant. It is, therefore, meaningful to compare the values of tempera-

tures obtained at different values of the impact parameter.

When temperatures are extracted from the characteristics of the emitted fragments, one must clearly identify the source of these fragments. Here, we mainly use the method of double ratios of isotope yields [15] with cross checks from the relative population of particle unstable states [16]. Both methods require that the considered fragments are emitted from the same source. Therefore, from the experimental point of view, one has to adopt a procedure of data analysis which allows to identify the emitting system and assures that all the selected fragments come from this system. For this purpose we selected events for a given range of impact parameter and verified that the selected fragments were emitted from a unique nearly isotropic source as expected for thermal equilibrium. Finally we fit the energy spectra of each isotope by a Maxwellian distribution in the rest frame of the emitting source.

The method of double ratios of isotope yields [15], which has been extensively used in the last years in many HI experiments, is based on the following strong assumptions: (i) free nucleons and composite fragments are contained within a certain volume V at a single temperature T and are in thermal equilibrium; (ii) it is possible to use the Maxwell-Boltzmann statistics; (iii) the system has reached the chemical equilibrium; (iv) the experimental yield of a fragment is proportional to its density inside the volume V; (v) all detected nuclei originate from a single source. The double ratio R of the yields Y of four isotopes in their ground states, prior to secondary decay is then given by

$$R=\frac{Y(A_1,Z_1)/Y(A_1+1,Z_1)}{Y(A_2,Z_2)/Y(A_2+1,Z_2)}=\frac{e^{B/T}}{a}, \tag{1}$$

where a is a constant related to spin and mass values and

$$B=BE(Z_1,A_1)-BE(Z_1,A_1+1)$$
$$-BE(Z_2,A_2)+BE(Z_2,A_2+1),$$

and $BE(Z,A)$ is the binding energy of a nucleus with charge Z and mass A [15]. Similarly, the ratio of yields Y of two states of a given fragment, prior to secondary decay, are given by the equation

$$R_{ij}=\frac{Y_i}{Y_j}=\frac{2J_i+1}{2J_j+1}e^{-(E_i^*-E_j^*)/T}, \tag{2}$$

where the E^* and J are the excitation energy and spin of the respective states [16,17].

In principle, the temperature dependences of the isotope ratio R and excited state ratio R_{ij} allow for determinations of the temperature T. However, the fragments can be highly excited and then secondary decays from higher lying states of the same and heavier nuclei can lead to non-negligible corrections to the measured ratios R and R_{ij} [16,19]. To reduce the sensitivity to such corrections, it is advisable to choose cases for which $B \gg T$ and $E_i^*-E_j^* \gg T$ since the uncertainties on T are proportional to T/B and to $T/(E_i^*-E_j^*)$, respectively.

In Ref. [18] the ^{36}Ar+^{197}Au reaction at 35 MeV/nucleon was studied and the temperatures of the systems formed in central collisions were extracted, both from isotope yields and from excited states populations. The two methods gave consistent temperatures values of about 4 MeV after correction for secondary decay. These values were consistent with published data concerning the caloric curve [6,8]. In this paper we verified the consistency of the two methods for the central Au+Au 35 MeV/nucleon collisions. Then, for peripheral collisions, we used only the double ratio of isotope yields technique. Some results of these measurements and of this procedure have already been published [20].

IV. RESULTS AND DISCUSSION

A. Central collisions

We define central collisions by the cut $\hat{b}=b/b_{max}<0.3$ ($b_{max}\simeq 14$ fm). For the events satisfying this condition, in the HAG experiment we measured the light isotopes with good mass resolution (see Fig. 1) and in the LAG experiment all the fragments (until the heaviest produced) were detected with good atomic-number resolution, allowing us to study the multifragmentation of the nuclear systems formed in these central collisions. The analysis of the data collected in the HAG experiment was made with the aim of measuring the temperatures of the systems observed in the LAG experiment and undergoing multifragmentation.

We briefly recall the relevant results obtained in the LAG measurements, already published for central Au+Au 35 MeV/nucleon collisions [21–23]. Several exclusive experimental observables indicated that the observed multifragment emission is due to the decay of a unique equilibrated system [21]. In the framework of a Monte Carlo many-body Coulomb trajectory calculation, fragment emission was found compatible with a near isotropic decay of a source consisting of more than 300 nucleons, of diluted nuclear density, $\rho\simeq\rho_0/4$, and life-time smaller than 100 fm/c. A possible contribution of collective energy, as, e.g., radial flow, is lower than 1 MeV/nucleon [22]. The contribution to the multifragmentation cross section coming from the decay of projectile and targetlike residues was found to be negligible. Comparing the data with a microcanonical statistical multifragmentation model (SMM) [24], fragment emission was shown [23] to be consistent with the statistical breakup of a single source having $Z=126$–138, $A=315$–343, $\rho\simeq\rho_0/6-\rho_0/3$, and an excitation energy $E^*/A\approx 5$–6 MeV. These main source characteristics are compatible with predictions of dynamical models based on the Boltzmann Nordheim Vlasov equation. In the mean field approximation and with a soft equation of state for an impact parameter of 1 fm after 80 fm/c from the initial stage of the reaction we have an equilibrated system with mass ≈ 324, charge ≈ 136, nuclear density $\approx\rho_0/2$, and an excitation energy of ≈ 6 MeV/nucleon. The experimental data and their comparison with models indicate that in central collisions a unique equilibrated source is formed. This result confirms that the basic hypothesis for extracting temperatures from the isotope yield ratio seems to be satisfied.

To be sure that the light isotopes detected in the HAG experiment were emitted from the unique and equilibrated fragment source observed in the LAG experiment, the choice of the events was made by first imposing constraints on Nc

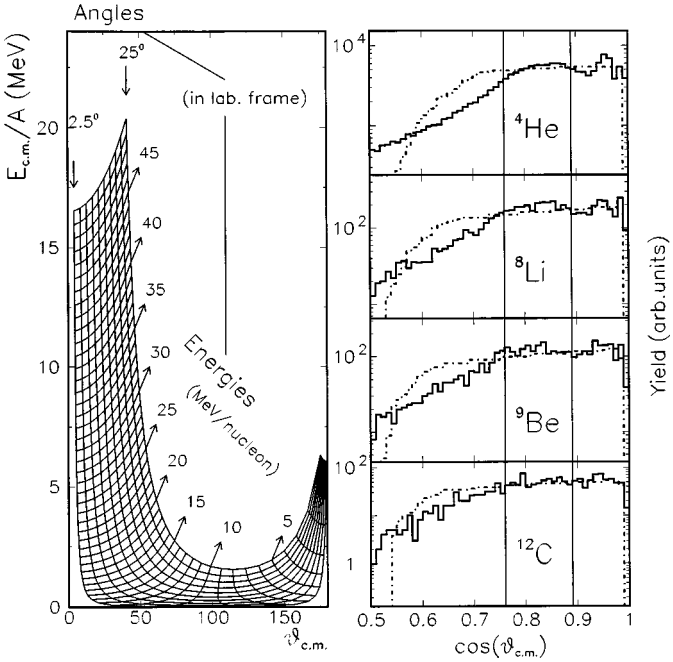

FIG. 2. Angular distributions for central collisions: detection efficiency for MULTICS array and for different emission energies and angles (calculation related to a mass $A=4$ are shown) and experimental data for some isotopes. Full line: experimental distributions, dashed line: simulation (see text). The vertical lines show the angular range chosen for the temperature analysis.

(same impact parameter interval as in the LAG measurements, $\hat{b}<0.3$) and then accurately inspecting the angular distributions and the energy spectra of all the detected isotopes in the center of mass of their source.

A difficulty in assessing the isotropy and the Maxwellian shape of the energy spectra results from the fact that isotopic resolution was only obtained over a limited angular range (MULTICS array). Angular distributions and energy are thus distorted by the acceptance of the apparatus. To evaluate these distortions, a fragment source isotropically emitting in its c.m. frame was simulated and the calculated angular and energy distributions of its products were filtered by the acceptance of the apparatus. For angles in the c.m. larger than 40°, both angular and energy distributions are strongly distorted by the acceptance (left panel of Fig. 2). For smaller angles the distortions are less important and are of the order of 20% at maximum, with respect to an isotropic distribution (Fig. 2). Therefore we analyzed the central collisions events looking at the angular distribution of the isotopes in the angular range up to 40° in the c.m. frame. For fragments with charge $Z>2$, the angular distributions are consistent with isotropic emission of a single source moving with the center of mass velocity, while the H isotopes and α particles show some enhancement at $\theta_{\mathrm{c.m.}}<20°$ which may reflect contributions due to preequilibrium emission (right panel of Fig. 2). This contamination could affect the values of the temperatures extracted from ratios involving H and He isotopes. Therefore a further event selection has been made: only the events in the angular range $30°<\theta_{\mathrm{c.m.}}<40°$ have been considered, where this contamination appears to be negligible.

TABLE I. Temperature parameters extracted from a Maxwellian fit procedure of the isotope energy spectra for central (T^c_{slope}) and peripheral ($0.7<\hat{b}<0.8$ case) (T^p_{slope}) collisions.

Z	A	T^c_{slope} (MeV)	T^p_{slope} (MeV)
1	1	4.1±0.5	4.2±0.5
1	2	8.7±0.5	4.6±0.5
1	3	10.2±0.5	4.8±0.5
2	3	14.6±1.5	10.7±1.5
2	4	12.0±0.5	8.6±0.5
2	6	15.0±1.5	10.6±1.5
3	6	16.9±1.5	13.7±1.5
3	7	18.3±1.5	15.8±1.5
3	8	18.9±1.5	16.0±1.5
4	7	18.4±2.0	15.7±2.0
4	9	16.3±1.5	15.8±1.5
4	10	15.7±2.0	14.1±2.0
5	10	17.4±2.0	13.6±2.0
5	11	15.4±1.5	13.6±1.5
5	12	16.8±2.0	13.0±2.0
6	12	20.6±2.0	18.6±2.0
6	13	21.2±2.0	19.4±2.0

To further check the equilibration of the emitting source, we looked at the energy distributions in the c.m. frame for different isotopes. The energy distributions can be strongly influenced by the fact that Coulomb and collective energies are mass dependent; in this case energy spectra of different isotopes may display different slopes. On the contrary, the thermal energy contribution has to be the same for all masses. By fitting energy distributions with a Maxwellian function (for a surface emission)

$$Y(E)=\frac{(E-E_0)}{T^2_{slope}}\cdot e^{-(E-E_0)/T_{slope}} \tag{3}$$

we got similar values for the parameter related to the apparent temperatures T_{slope}, while the Coulomb repulsion, E_0, was fixed for all isotopes at fixed atomic number Z corresponding to a source with $\rho=1/6$ and $Z=126$ and $A=315$ (Fig. 3 and Table I). We used E_0 values calculated for surface and volume emission at different nuclear densities, and obtained the same trend for the T_{slope} values. The fact that T_{slope} values are higher than those extracted from isotope ratio or level population ratios can be explained mainly in terms of Fermi-motion of nucleons [25] and variations in the Coulomb barrier depending on the point of emission within the system. Differences in T_{slope} values for different Z fragments can be explained in terms of a Coulomb driven multifragment decay [21]. As it appears in Table I some anomalous behavior is observed for H and He isotopes: the extracted values of T_{slope} exhibit a mass dependence which is large for protons and smaller for He particles. Possibly, this might be attributed to some remaining contamination from pre-equilibrium emission and sequential decay. On the other hand it should be stressed that the care in selecting the events (angular selection) makes negligible the ^{4}He ''background'' contribution from pre-equilibrium; contribution from secondary decays can still remain. Then for tempera-

TABLE II. Temperatures extracted from different double yield isotope ratio (T_{exp}) and calculated values after sequential feeding correction (T_{corr}).

	$\hat{b}$	T_{exp} (MeV)	T_{corr} (MeV)		$\hat{b}$	T_{exp} (MeV)	T_{corr} (MeV)
^{3}He/^{4}He-^{6}Li/^{7}Li	>0.95	4.03±0.12	4.01±0.11	^{6}Li/^{7}Li-^{11}C/^{12}C	0.7–0.8	4.66±0.26	3.76±0.21
^{3}He/^{4}He-^{7}Li/^{8}Li	>0.95	3.24±0.06	3.62±0.07	^{7}Li/^{8}Li-^{11}C/^{12}C	0.7–0.8	3.62±0.11	4.02±0.12
^{3}He/^{4}He-^{9}Be/^{10}Be	>0.95	5.22±0.28	3.67±0.20	^{9}Be/^{10}Be-^{11}C/^{12}C	0.7–0.8	7.02±0.65	3.86±0.36
^{3}He/^{4}He-^{11}B/^{12}B	>0.95	3.49±0.15	3.71±0.16	^{11}B/^{12}B-^{11}C/^{12}C	0.7–0.8	3.91±0.17	3.95±0.17
^{3}He/^{4}He-^{12}C/^{13}C	>0.95	3.65±0.15	3.71±0.15	^{11}C/^{12}C-^{12}C/^{13}C	0.7–0.8	4.02±0.20	3.92±0.20
^{3}He/^{4}He-^{13}C/^{14}C	>0.95	3.21±0.17	3.39±0.18				
^{6}Li/^{7}Li-^{11}C/^{12}C	>0.95	5.30±0.74	4.17±0.58	^{3}He/^{4}He-^{6}Li/^{7}Li	0.6–0.7	4.88±0.05	4.85±0.05
^{7}Li/^{8}Li-^{11}C/^{12}C	>0.95	3.53±0.24	3.92±0.27	^{3}He/^{4}He-^{7}Li/^{8}Li	0.6–0.7	3.89±0.03	4.47±0.03
^{9}Be/^{10}Be-^{11}C/^{12}C	>0.95	7.30±1.58	3.94±0.85	^{3}He/^{4}He-^{9}Be/^{10}Be	0.6–0.7	6.94±0.15	4.44±0.10
^{11}B/^{12}B-^{11}C/^{12}C	>0.95	3.91±0.42	3.96±0.43	^{3}He/^{4}He-^{11}B/^{12}B	0.6–0.7	4.06±0.05	4.35±0.05
^{11}C/^{12}C-^{12}C/^{13}C	>0.95	4.20±0.49	4.10±0.48	^{3}He/^{4}He-^{12}C/^{13}C	0.6–0.7	4.25±0.06	4.34±0.07
				^{3}He/^{4}He-^{13}C/^{14}C	0.6–0.7	4.15±0.08	4.46±0.08
^{3}He/^{4}He-^{6}Li/^{7}Li	0.9–0.95	4.22±0.09	4.19±0.09	^{6}Li/^{7}Li-^{11}C/^{12}C	0.6–0.7	4.91±0.20	3.93±0.16
^{3}He/^{4}He-^{7}Li/^{8}Li	0.9–0.95	3.29±0.05	3.69±0.06	^{7}Li/^{8}Li-^{11}C/^{12}C	0.6–0.7	3.82±0.09	4.28±0.10
^{3}He/^{4}He-^{9}Be/^{10}Be	0.9–0.95	5.09±0.21	3.60±0.15	^{9}Be/^{10}Be-^{11}C/^{12}C	0.6–0.7	7.46±0.51	3.98±0.27
^{3}He/^{4}He-^{11}B/^{12}B	0.9–0.95	3.53±0.11	3.75±0.13	^{11}B/^{12}B-^{11}C/^{12}C	0.6–0.7	3.98±0.12	4.03±0.12
^{3}He/^{4}He-^{12}C/^{13}C	0.9–0.95	3.94±0.14	4.02±0.15	^{11}C/^{12}C-^{12}C/^{13}C	0.6–0.7	4.19±0.16	4.09±0.15
^{3}He/^{4}He-^{13}C/^{14}C	0.9–0.95	3.35±0.13	3.55±0.14				
^{6}Li/^{7}Li-^{11}C/^{12}C	0.9–0.95	4.71±0.50	3.80±0.40	^{3}He/^{4}He-^{6}Li/^{7}Li	0.5–0.6	5.05±0.06	5.01±0.06
^{7}Li/^{8}Li-^{11}C/^{12}C	0.9–0.95	3.39±0.19	3.75±0.21	^{3}He/^{4}He-^{7}Li/^{8}Li	0.5–0.6	4.10±0.03	4.74±0.03
^{9}Be/^{10}Be-^{11}C/^{12}C	0.9–0.95	6.01±0.90	3.53±0.53	^{3}He/^{4}He-^{9}Be/^{10}Be	0.5–0.6	7.74±0.19	4.75±0.12
^{11}B/^{12}B-^{11}C/^{12}C	0.9–0.95	3.70±0.30	3.74±0.30	^{3}He/^{4}He-^{11}B/^{12}B	0.5–0.6	4.24±0.06	4.56±0.06
^{11}C/^{12}C-^{12}C/^{13}C	0.9–0.95	4.25±0.42	4.15±0.41	^{3}He/^{4}He-^{12}C/^{13}C	0.5–0.6	4.38±0.07	4.48±0.07
				^{3}He/^{4}He-^{13}C/^{14}C	0.5–0.6	4.47±0.09	4.83±0.10
^{3}He/^{4}He-^{6}Li/^{7}Li	0.8–0.9	4.42±0.08	4.39±0.08	^{6}Li/^{7}Li-^{11}C/^{12}C	0.5–0.6	4.85±0.20	3.89±0.16
^{3}He/^{4}He-^{7}Li/^{8}Li	0.8–0.9	3.46±0.04	3.91±0.04	^{7}Li/^{8}Li-^{11}C/^{12}C	0.5–0.6	3.93±0.09	4.41±0.10
^{3}He/^{4}He-^{9}Be/^{10}Be	0.8–0.9	5.60±0.19	3.85±0.13	^{9}Be/^{10}Be-^{11}C/^{12}C	0.5–0.6	7.91±0.59	4.11±0.31
^{3}He/^{4}He-^{11}B/^{12}B	0.8–0.9	3.66±0.09	3.90±0.09	^{11}B/^{12}B-^{11}C/^{12}C	0.5–0.6	4.05±0.13	4.10±0.13
^{3}He/^{4}He-^{12}C/^{13}C	0.8–0.9	3.88±0.10	3.95±0.10	^{11}C/^{12}C-^{12}C/^{13}C	0.5–0.6	4.18±0.16	4.08±0.16
^{3}He/^{4}He-^{13}C/^{14}C	0.8–0.9	3.75±0.12	4.00±0.13				
^{6}Li/^{7}Li-^{11}C/^{12}C	0.8–0.9	4.71±0.35	3.80±0.28	^{3}He/^{4}He-^{6}Li/^{7}Li	<0.3	4.68±0.07	4.64±0.07
^{7}Li/^{8}Li-^{11}C/^{12}C	0.8–0.9	3.49±0.14	3.87±0.15	^{3}He/^{4}He-^{7}Li/^{8}Li	<0.3	4.03±0.04	4.65±0.04
^{9}Be/^{10}Be-^{11}C/^{12}C	0.8–0.9	6.32±0.71	3.63±0.41	^{3}He/^{4}He-^{9}Be/^{10}Be	<0.3	7.10±0.19	4.50±0.14
^{11}B/^{12}B-^{11}C/^{12}C	0.8–0.9	3.72±0.21	3.76±0.22	^{3}He/^{4}He-^{11}B/^{12}B	<0.3	4.04±0.06	4.14±0.06
^{11}C/^{12}C-^{12}C/^{13}C	0.8–0.9	3.98±0.26	3.89±0.26	^{3}He/^{4}He-^{12}C/^{13}C	<0.3	4.09±0.07	4.33±0.07
				^{3}He/^{4}He-^{13}C/^{14}C	<0.3	4.03±0.08	4.17±0.08
^{3}He/^{4}He-^{6}Li/^{7}Li	0.7–0.8	4.60±0.07	4.57±0.07	^{6}Li/^{7}Li-^{11}C/^{12}C	<0.3	4.73±0.22	3.81±0.18
^{3}He/^{4}He-^{7}Li/^{8}Li	0.7–0.8	3.67±0.03	4.18±0.04	^{7}Li/^{8}Li-^{11}C/^{12}C	<0.3	4.00±0.11	4.50±0.11
^{3}He/^{4}He-^{9}Be/^{10}Be	0.7–0.8	6.47±0.19	4.24±0.12	^{9}Be/^{10}Be-^{11}C/^{12}C	<0.3	7.84±0.64	4.09±0.33
^{3}He/^{4}He-^{11}B/^{12}B	0.7–0.8	3.95±0.07	4.22±0.07	^{11}B/^{12}B-^{11}C/^{12}C	<0.3	4.00±0.14	4.05±0.14
^{3}He/^{4}He-^{12}C/^{13}C	0.7–0.8	4.05±0.08	4.13±0.08	^{11}C/^{12}C-^{12}C/^{13}C	<0.3	4.05±0.17	3.96±0.17
^{3}He/^{4}He-^{13}C/^{14}C	0.7–0.8	3.90±0.10	4.18±0.11				

ture measurements the present analysis allows us to use all the isotopes, except for those of the H for which contaminations can affect the isotope ratio. The remaining contribution from secondary decays to the ^{4}He yield will be corrected as explained at the end of this paragraph. It is worthwhile to note that the energy spectra of ^{3}He and ^{6}He show an identical shape (same E_0 and same T_{slope}) and that it is the ^{4}He spectrum which is slightly different. This small difference of the ^{4}He energy distribution might be interpreted as an indication of a later emission of ^{4}He with respect to the other isotopes [26]. Moreover, as collective energies are mass dependent while the thermal energy is not, the identity of the energy spectra of ^{3}He-^{6}He is a strong indication of the absence of important collective motions in this reaction.

The results on the angular and energy analysis of the events confirm that the conditions of equilibration of the isotope source seem to be satisfied and that the isotope ratios method to extract temperatures can be applied.

Once the set of data coming from a single source is defined, the good isotopic resolution (up to carbon) allows the extraction of temperatures from a high number of isotope ratios (41).

Figure 4 shows isotope-ratio temperatures as a function of B [see Eq. (1)]. The best thermometers are those that deal

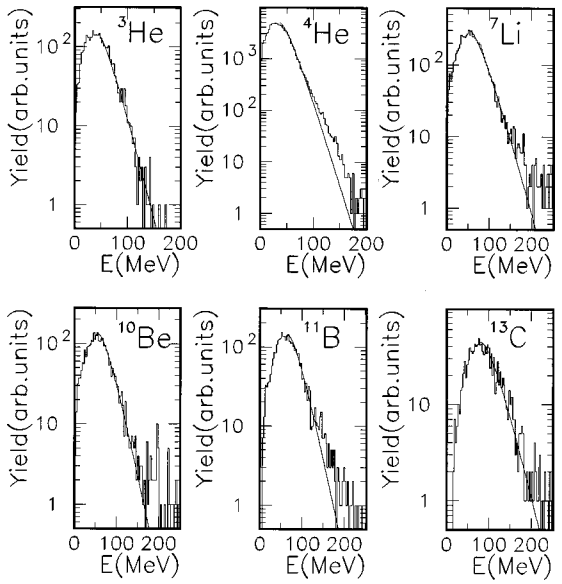

FIG. 3. Energy distributions and Maxwellian fit for different isotopes in central collisions.

with yields of isotopes with large difference in the ground state binding energies; in fact for large B values we observe that the extracted temperatures tend towards a value of about 4 MeV. Figure 5(g) and Table II give the values for 12 thermometers with $B>9$ MeV (open circles). While event selection is different from our previous work [20] the present results are consistent. In addition to the previously studied ratios involving ^{3}He/^{4}He, the present work includes heavier-isotope double ratios ^{6}Li/^{7}Li-^{11}C/^{12}C, ^{7}Li/^{8}Li-^{11}C/^{12}C, ^{9}Be/^{10}Be-^{11}C/^{12}C, ^{11}B/^{12}B-^{11}C/^{12}C, ^{11}C/^{12}C-^{12}C/^{13}C, which give completely compatible results. The errors of the temperatures obtained with the ^{11}C thermometers are larger than the others because of the very low yield of this isotope. Besides the statistical errors we evaluated the uncertainties due to the overall background and the possible ^{12}C contamination of the ^{11}C yield. This contamination of the ^{11}C yield is estimated to be less than 10% and contributes to the systematic error of the temperature determination by less than 3%.

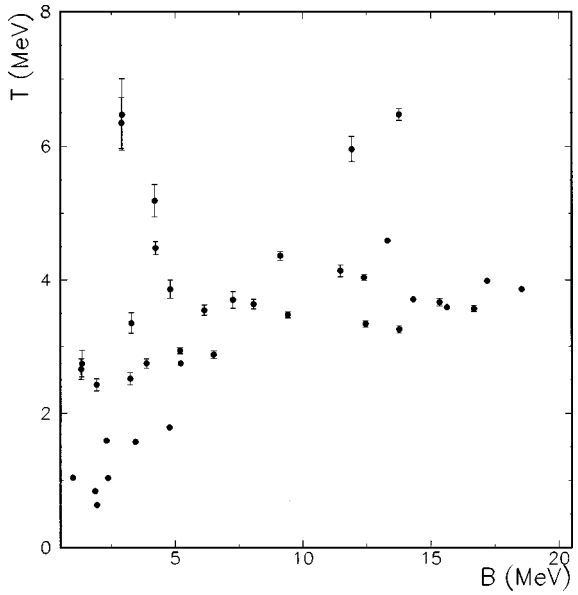

FIG. 4. Temperature extracted from different isotope thermometers as a function of the B parameter [15] for central collisions.

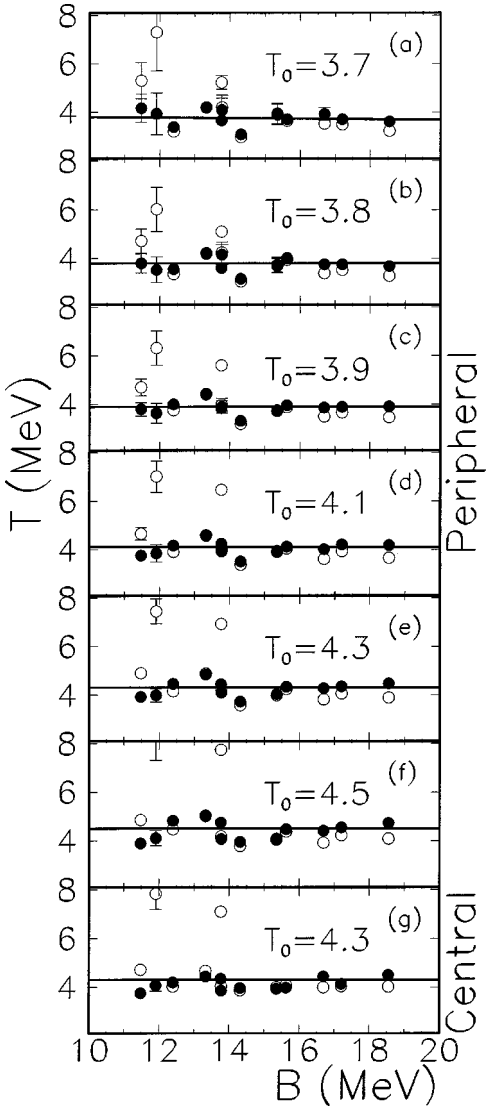

FIG. 5. Temperature extracted [(a)–(f) peripheral collisions; (g) central], from the ''best'' isotope thermometers as a function of the B parameter [15], from experimental data (open points) and after correction for sequential decay feeding [19,27] (solid circles).

The fluctuations in the temperature obtained from different thermometers are likely due to secondary decays of highly excited fragments. As explained in Ref. [16] sequential decay calculations, to evaluate the modification to the initial distributions due to the particle whose decay feeds the measured yields, were used. In these calculations the excited states of primary emitted fragments are assumed to be thermally populated; unknown spins and parities of low lying discrete states were assigned randomly and the calculations were repeated to assess the sensitivities of the population probabilities to these spectroscopic uncertainties. For the isotope ratios involving ^{11}C an empirical procedure was used as explained in Refs. [19,27]. It was then possible to use empirical correction factors to strongly reduce these fluctuations; this correction procedure is described in Refs. [19,27]

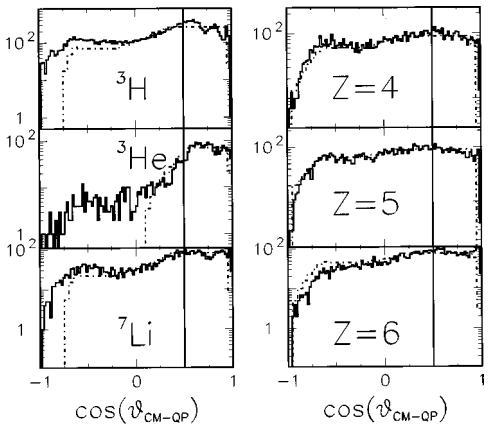

FIG. 6. Angular distributions for events falling in the range of impact parameter $0.7<\hat{b}<0.8$ [full line, experimental data; dot-dashed line, calculated values from simulation ($v_{QP}=6.7$ cm/ns)]. The vertical line show the angular range chosen for the temperature analysis.

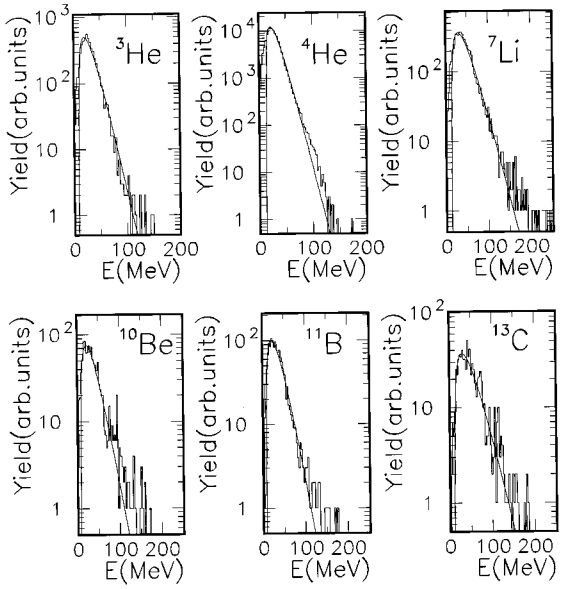

FIG. 7. Energy distributions and Maxwellian fit for different isotopes in peripheral collisions.

where it has been shown for temperatures in the neighborhood of about 4 MeV that the correction factors do not depend strongly on the reaction or on the decaying system [19]. The corrected temperature values are plotted in Fig. 5(g) (full circles) and reported in Table II.

The calculations are made assuming a temperature T_0 of the emitting source; we were able to reproduce all the temperatures measured with the 12 thermometers starting from a value of 4.3 ± 0.4 MeV. The present value can be assumed as the breakup temperature T_0 of the large size nuclear system formed in central collisions. This result is in agreement with the slightly higher value of 4.4 ± 0.2 [20] obtained from the family of the ^{3}He/^{4}He thermometers. SMM calculations which describe the present data [23] require an excitation energy of $E^*/A\approx5$–6 MeV. This pair of values ($E^*\approx5$–6 MeV/nucleon; $T_0=4.3$) is compatible with the existing data for the caloric curve [6,8] which give a temperature value between 4 and 5 MeV in this excitation energy range.

The isotope ratio temperatures are compared to those obtained from the method of the excited states of ^{5}Li, ^{4}He, and ^{10}B [20]. We find good agreement between the excited state temperature of $T=4.2\pm0.6$ MeV and the current temperature of $T=4.3\pm0.4$ MeV. At the present excitation energies this consistency suggests that the local thermal equilibrium of the system formed in very central collisions is attained, and shows that the collective motions, if present, are negligible, and that the corrections, introduced to take into account the sequential decay of the fragments in the case of the isotope yield ratio method, are reliable.

B. Peripheral collisions

The regime $\hat{b}>0.5$ was investigated with a focus on fragments emitted from the quasiprojectile (QP) system. To remove reaction products coming from quasitarget or neck emission, we analyzed the events for 6 different $\hat{b}$ intervals (see first column of Table III) with the additional selection of isotopes which have a velocity component parallel to the beam larger than 5 cm/ns in the laboratory frame (the velocity of the beam is 8.2 cm/ns). Furthermore, in order to select events coming from the QP disassembly we simulated a source emitting isotropically in the c.m. of the QP. The simulated distributions were filtered by the acceptance of the apparatus. Since different velocities of the QP source yield different angular and energy experimental distributions in the c.m. of the QP, a best fit to the experimental distribution of all isotopes from H to C was used to extract the velocity of the QP emitting source (v_{QP}) for each cut on impact parameter (see the second column of Table III). As may be expected v_{QP} decreases going from peripheral towards midperipheral collisions (Table III). This decrease in QP velocity is directly related to an increase on excitation energy of the emitting QP source. It should be noted that a unique v_{QP} for each selected impact parameter reproduces the experimental angular distribution of each isotope, consistent with the notion that all the isotopes come from the same source.

The simulations indicate that distortions in the angular distribution, due to detection inefficiencies, are negligible in the range up to 60° in the QP c.m. frame. Figure 6 gives an example of the experimental (full lines) and simulated (dot-dashed lines) angular distribution for $v_{QP}=6.7$ cm/ns (best fit result) in the $0.7<\hat{b}<0.8$ case for different fragments.

In order to better check the selection of the emitting source we also studied the energy distributions of the emitted isotopes. As for the case of central collisions, the distributions have Maxwellian shapes, and the T_{slope} are similar (within errors) for all isotopes, except for H and He (see Table I and Fig. 7). Further the ^{3}He and ^{6}He energy spectra have similar shapes while the ^{4}He spectrum indicates a smaller T_{slope}. This holds for all cuts on impact parameter considered. Therefore, even in these cases, we have indications that the conditions of the equilibration of the fragmenting systems are satisfied. Starting from the obtained v_{QP} values we can fix an upper limit to the excitation energy (E^*_{ul}) of the source in a naive way using the energy conservation (Table III):

TABLE III. Velocities, excitation energies, isotopic temperatures, and breakup temperatures of the emitting sources for different impact parameter intervals.

$\hat{b}$	v_{source} (cm/ns)	E^*_{ul}/A (MeV/nucleon)	E^*_{Cal} (MeV/nucleon)	E^*_{SMM} (MeV/nucleon)	T_{iso} (MeV)	T_0 (MeV)
>0.95	7.2 ± 0.1	3.5	2.0 ± 0.7	2.2 ± 0.6	3.4	3.7 ± 0.2
0.9–0.95	7.0 ± 0.1	4.3	3.1 ± 1.0	3.6 ± 0.8	3.5	3.8 ± 0.2
0.8–0.9	6.9 ± 0.1	4.6	4.0 ± 1.1	4.2 ± 0.8	3.6	3.9 ± 0.2
0.7–0.8	6.7 ± 0.1	5.3	4.9 ± 1.3	4.9 ± 0.8	3.8	4.1 ± 0.2
0.6–0.7	6.5 ± 0.1	5.7	5.7 ± 1.2	5.5 ± 0.6	3.9	4.3 ± 0.2
0.5–0.6	6.3 ± 0.1	6.2	6.2 ± 1.1	5.9 ± 0.5	4.1	4.5 ± 0.2
<0.3				5.5 ± 0.5	4.0	4.3 ± 0.4

$$E^*_{ul}=\frac{1}{2}\left(\frac{1}{2}E_{beam}-m_{\mathrm{QP}}v'^2_{\mathrm{QP}}\right), \tag{4}$$

where m_{QP} has been chosen as the mass of a Au nucleus, v'^2_{QP} is the QP velocity in the center of mass frame and the factor 1/2 takes into account the projectile-target symmetry and the assumptions that on average there is an equal sharing of excitation energy between the two systems. In this way we completely neglect the excitation energy transferred to a neck or fireball system, if formed.

Excitation energies were estimated in two ways: (i) exploiting the measured energies and the observed mass of the reaction products in the complete events ($>80\%$ of the total charge and total momentum) recorded in the LAG experiment and making use of the calorimetric method [31]; (ii) assuming the equilibration of the emitting systems and using the SMM to describe the experimental findings of the fragment emission. In the first evaluation the QP was reconstructed as in Ref. [32] and its velocity was obtained from the study of fragment momentum distribution [22]. Within the experimental uncertainties the velocity values are the same as those obtained in the HAG measurements (listed in Table III) for the same impact parameter interval. The excitation energy of each system was, then, calculated summing up the kinetic energies of the charged particles, fragments and neutrons emitted from the considered nucleus in its frame and the Q value (energy difference between the initial and final masses), taking into account the mass and isospin conservation. The multiplicity of neutrons, not detected in the experiments, was calculated from the difference between the mass of each primary hot nucleus and the sum of its charged products. It was assumed that each neutron has a mean kinetic energy corresponding to the same temperature of other reaction products. The obtained values of the excitation energies per nucleon are listed in Table III.

The second excitation energy evaluation is similar to that used for central collisions: the statistical model SMM was used to describe the decay of the QP by fitting the measured charge distribution obtained from the LAG experiment and the best fit excitation energy was extracted as that of the emitting source. The calculation were made for a Au nucleus with one third normal density and excitation energies ranging from zero to 8 MeV/nucleon considering a flat energy distribution. The velocity of the fragment source was assumed as in the experimental case (changing from 8 to about 6 cm/ns, depending on the excitation energy). We stress that even if the excitation energy and Nc are on the average correlated, one has to take into account that for a given value of excitation energy Nc fluctuates in the exit channel of the reaction [28] and therefore one has to consider excitation energy intervals to reproduce data. The events generated by SMM for different input excitation energies were filtered by the apparatus. Only filtered SMM events satisfying the condition that at least 70% of the source charge had been detected were used for further analyses. Indeed this condition allows to observe (after the filter) an excitation energy distribution flat as the input one, so that the distortions introduced by the filter are small. Each experimental charge distribution was reproduced by properly choosing SMM excitation energy intervals. It was found that the minimum value of the excitation energy is fixed by the reproduction of the high tail of the charge distribution, while the upper value is fixed by the reproduction of the yield of light fragments. In Fig. 8 the experimental charge distributions and the corresponding SMM predictions are shown for the 6 impact parameter intervals. The predicted and experimental charge distributions were normalized to the number of events, so that the vertical scale of Fig. 8 represents both for the experimental data and for the SMM predictions the mean elemental multiplicity per event. As it can be seen from Fig. 8 the

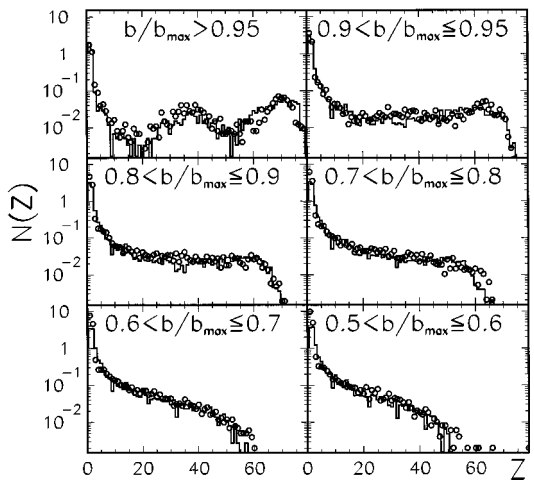

FIG. 8. Charge distributions for peripheral and midperipheral collisions (open point: experimental data; histogram: SMM predictions).

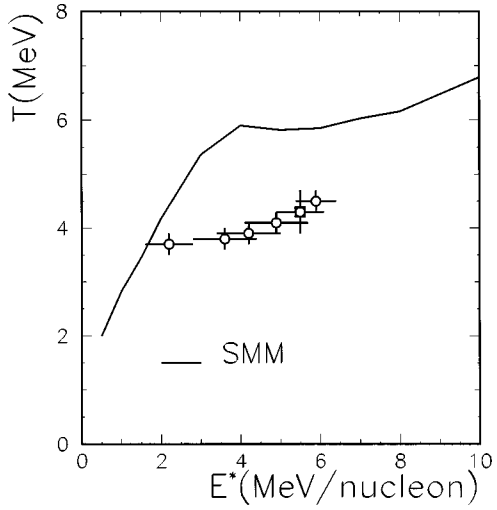

FIG. 9. Present experimental breakup temperature as a function of excitation energy (the open square is for central collisions); the solid curve represents the SMM predictions for the caloric curve.

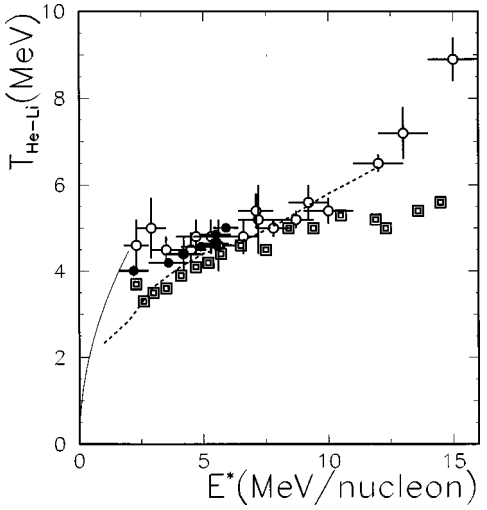

FIG. 10. Experimental caloric curve: open point, Ref. [6]; double squared open point, Ref. [8]; full point, present data (the full square is for the central collisions); the solid line represents the low-temperature approximation of a fermionic system for an inverse level density parameter of 10 MeV; the dashed line is related to double isotope temperature extracted starting from SMM predictions for a ^{197}Au source.

reproduction of all the spectra is very good.

In Table III the excitation energy ranges used to get agreement between SMM predictions and experimental data are summarized. Assuming less diluted sources, for fixed value of the temperature, the excitation energy must assume higher values, approaching the E^*_{ul} ones.

Within the uncertainties of the two procedures there is a good agreement between the values predicted by SMM and those obtained with the calorimetric method. In both evaluations the mass of the QP does not play an important role, since, when the excitation energy per nucleon is considered, all the quantities scale in the same way. As a check, we changed the mass of the decay system of a 20% and we did not find any noticeable difference in the E^*/A.

Finally, selecting events in the range $\theta_{\mathrm{QPCM}}<60°$, we extracted the temperatures of each system formed at different $\hat{b}$ by means of the isotope ratio method [Figs. 5(a)–5(f)]. As discussed in the previous section the best thermometers are those with high values of the B parameter; in Table III are reported the average values T_{iso} of the temperatures of the thermometers with highest B values. As in central collisions, the fluctuations in values extracted from different thermometers are attributed to secondary sequential decays of excited primary fragments, and they can be strongly reduced by means of empirical correction factors [19]. Using this procedure [19,27] the average breakup temperature T_0 has been obtained for each impact parameter interval. These values, listed in Table III, are slowly increasing with the excitation energy.

C. Discussion

In Fig. 9 the extracted breakup temperatures T_0 are plotted as a function of the excitation energy for which SMM predictions match the experimental charge distributions. They show a slow, continuous increase with excitation energy. Even considering the experimental uncertainties the temperature of the nuclear system formed at $0.5<\hat{b}<0.6$ is slightly higher than that of the ''central'' one, but even its excitation energy is slightly higher. This could be due to the fact that in the central collisions a small amount of energy (less than 1 MeV/nucleon) might be gone in some collective motion (e.g., radial flow). In Fig. 9 the present results are shown together with the predictions of the SMM for the freeze-out break-up temperatures (the open square refers to central collisions). The calculated values disagree with those extracted from the data both in magnitude and in the dependence on energy.

To have a comparison with the results of Refs. [6,8] we plotted in Fig. 10 the temperatures obtained with the ^{6}Li/^{7}Li-^{3}He/^{4}He thermometer ($T_{\mathrm{He,Li}}$) as a function of the excitation energy together with the results of the other measurements which used the same thermometer. It should be noted that the absolute T values in the three experimental results are obtained with different feeding correction prescriptions. It is interesting to note that the values of the temperature extracted in the present analysis and those extracted via the analyses of Refs. [6–8] are similar even though the present study was performed at a much lower bombarding energy. As far as the shape of the caloric curve is concerned, the present results show a slow monotonic increasing behavior, both for breakup T_0 and $T_{\mathrm{He,Li}}$ temperatures, similar to the trend of EOS data [8], rather than that indicated by the Aladin experiment [6]. However the present values are slightly higher than the EOS ones and closer to the Aladin data.

Moreover one has to note that the temperature extracted for the large and diluted emitting source formed in central collisions meets very well with the peripheral ones even if we are in presence of very different emitting systems. It appears that nuclear density, size, and Coulomb explosion have a small effect on the relationship between excitation energy and temperature.

In Fig. 10 the caloric curve predicted by the SMM for $T_{\mathrm{He,Li}}$ (taking into account the secondary decays) is also shown. It appears that the values of the isotope temperatures

are similar, but the experimental decreasing at lower excitation energies is much slower than the predicted one. It should be noted that, while this model predicts the existence of a plateau in the caloric curve when the initial temperature is considered, this plateau vanishes when the temperatures is that obtained with the isotope ratios. Moreover the SMM predictions for $T_{\mathrm{He,Li}}$ are smaller than the initial temperature, in fair agreement with the experimental data. The reason is that the isotope temperature predicted by SMM reflects secondary deexcitations of primary hot fragments whose excitation is smaller than the initial of the system, e.g., for initial excitation energy of 5 MeV/nucleon the average excitation of fragments is around 3 MeV/nucleon. In addition the secondary breakup gives a ''cooling effect'' providing an additional temperature decrease. All these effects are consequences of the energy conservation law included in the SMM model and disregarded in original treatment of Ref. [15] for the isotope ratio temperature. Therefore we must take into account that, according to SMM predictions, the temperature of the system at the break-up moment could be around 6 MeV even if the experimental extracted one is of the order of 4.5 MeV.

Very recently [28–30] there has been a further theoretical effort to study the caloric curve of finite systems. Though the calculations be based on different theoretical approach (finite temperature Thomas-Fermi theory, dynamic statistical model, SMM), all these studies predict a liquid-gas phase transition in the excitation energy range 4–10 MeV/nucleon and for temperatures of the order of 5–6 MeV. In Ref. [29] the authors discuss also the possibility that the presence of a collective radial flow leads the systems to move from a continuous phase transition to a sharp first order phase transition. They relate the presence of a plateau in the Aladin results to a possible compression of the system.

In Refs. [9,33] we showed that in the same reaction (LAG experiment) the peripheral events, in which the largest fragment has a velocity along the beam axis larger or equal to 75% of the beam velocity, present signals compatible with the presence of a liquid-gas phase transition near the critical temperature. Since the 75% of the beam velocity is 6.2 cm/ns, all the events here considered for $\hat{b}>0.5$ satisfy this condition and, therefore, if that phase transition is really present, we may argue that the temperature of the most excited system formed in the peripheral collisions could be very close to the critical temperature.

Moreover, it has to be noted that within the framework of classical molecular dynamics model (CMD) [33], which predicts critical behaviors, the reaction Au+Au at 35 MeV/nucleon leads to a formation of a system undergoing a liquid-gas phase transition just around $\hat{b}=0.5$–0.8 [33]. From the experimental point of view we can say that (i) we measured the temperature of the system formed in midperipheral collisions, (ii) it was observed that this system seems to present signals compatible with criticality [9], and (iii) its temperature is about 4.5 MeV and its excitation energy is around 6 MeV/nucleon.

V. CONCLUSIONS

In the study of the Au+Au 35 MeV/nucleon reaction it has been possible to investigate the characteristics of two different types of emitting sources: the unique one with a very large size formed in central collisions and six quasiprojectile sources having different excitation energies in peripheral ones. All these sources emit several light and intermediate mass fragments. The experimental angular and energy distributions of these fragments and model calculations indicate that these sources have reached a thermal equilibrium and that they are in conditions similar to those observed in the multifragmentation of the projectile in peripheral collisions at higher energies. We measured the temperatures of these emitting systems with a high number of isotopes ratios (41). The best thermometers are those with a high value of the B parameter of Eq. (1), therefore we used only those with $B>10$ MeV. In this way we had 12 measurements of the temperature for each nuclear system, 5 of which do not use the ^{3}He/^{4}He ratio, but involve heavier isotopes for which the problem of pre-equilibrium contamination is expected to be less important. The values of these temperatures have been corrected empirically for secondary decays and a very good agreement has been found for all the 12 corrected temperatures.

For central collisions the temperature of the system has been also measured with the population of excited states of ^{5}Li, ^{4}He, and ^{10}B; good agreement was found between the results obtained with these different techniques. In the study of peripheral and midperipheral collisions we observed that the temperatures of the QP disassembling systems are slowly increasing going towards smaller impact parameter. We also investigated the excitation energy of these six QP systems by means of a calorimetric measurement and of a comparison with SMM model in order to get information on the caloric curve of the finite nuclear matter.

First of all we noted that the peripheral collision results are consistent with those extracted for the large system formed in central collisions. This suggests that the relationship between temperature and excitation energy seems to depend weakly on detailed characteristics of the emitting source (such as nuclear density and size).

Moreover, we compared our data to those obtained by the Aladin and EOS Collaborations for the QP system at much higher energies; the values of the temperatures are in fair overall agreement. Our data indicate a slow increase of the temperature with the excitation energy, qualitatively similar to the EOS results. This increase has been interpreted by the EOS collaboration in forms of a continuous phase transition near the critical point.

The predictions of a statistical model (SMM) for the $T_{\mathrm{He,Li}}$ vs E^*/nucleon curve are in fair agreement with experimental data, however this model gives higher values for the freeze-out temperatures.

For the present reaction model calculations (CMD) suggest that for midperipheral collisions there should be the occurrence of a liquid-gas phase transition; theoretical statistical model (SMM) predict that a phase transition will occur for systems having excitation energies around 5–6 MeV/nucleon, in rough correspondence to the value experimentally extracted for the system investigated. Previous experimental results showed the possible presence of signals compatible with criticality for systems formed in these collisions. We measured the temperature of these systems and, if the phase transition really occurs near the critical point,

then the extracted breakup temperature should be close to the critical one.

ACKNOWLEDGMENTS

The authors are indebted to R. Bassini, C. Boiano, S. Brambilla, G. Busacchi, A. Cortesi, and M. Malatesta for their skillful assistance. One of us (P.F.M.) thanks the Consorzio Padova Ricerche for financial support. This work was supported in part by grants of the Italian Ministry of University and Scientific and Technological Research (MURST) and in part by the National Science Foundation under Grant No. PHY-95-28844.

[1] U. Mosel *et al.*, Nucl. Phys. **A236**, 252 (1974); G. Sauer *et al.*, *ibid.* **A264**, 221 (1976); H. R. Jaqaman *et al.*, Phys. Rev. C **27**, 2782 (1983); **29**, 2067 (1984).
[2] A. D. Panagiotou *et al.*, Phys. Rev. Lett. **52**, 496 (1984); J. E. Finn *et al.*, *ibid.* **49**, 1321 (1982); B. Jakobsson *et al.*, Z. Phys. A **307**, 293 (1982); B. Jakobsson *et al.*, Nucl. Phys. **A509**, 195 (1990); L. G. Moretto, Annu. Rev. Nucl. Part. Sci. **43**, 379 (1993).
[3] M. E. Fisher, Rep. Prog. Phys. **30**, 615 (1967).
[4] D. H. Gross, Phys. Rev. Lett. **56**, 1544 (1986); Rep. Prog. Phys. **53**, 605 (1990); Phys. Rep. **257**, 133 (1995).
[5] J. P. Bondorf *et al.*, Nucl. Phys. **A444**, 460 (1986).
[6] J. Pochodzalla *et al.*, Phys. Rev. Lett. **75**, 1040 (1995).
[7] J. B. Elliot *et al.*, Phys. Rev. C **49**, 3185 (1994); M. L. Gilkes *et al.*, Phys. Rev. Lett. **73**, 1590 (1994).
[8] J. A. Hauger *et al.*, Phys. Rev. Lett. **77**, 235 (1996); J. A. Hauger *et al.*, Phys. Rev. C **57**, 764 (1998); the data for the caloric curve were kindly supplied by B. Srivastava.
[9] P. F. Mastinu *et al.*, Phys. Rev. Lett. **76**, 2646 (1996); L. Phair *et al.*, *ibid.* **79**, 3538 (1997).
[10] Y. G. Ma *et al.*, Phys. Lett. B **390**, 41 (1997).
[11] R. T. de Souza *et al.*, Nucl. Instrum. Methods Phys. Res. A **295**, 109 (1990).
[12] I. Iori *et al.*, Nucl. Instrum. Methods Phys. Res. A **325**, 458 (1993).
[13] C. Cavata *et al.*, Phys. Rev. C **42**, 1760 (1990).
[14] C. Williams *et al.*, Phys. Rev. C **55**, R2132 (1997).
[15] S. Albergo *et al.*, Nuovo Cimento A **89**, 1 (1985).
[16] T. K. Nayak *et al.*, Phys. Rev. C **45**, 132 (1992); F. Zhu *et al.*, *ibid.* **52**, 784 (1995).
[17] D. J. Morrissey *et al.*, Annu. Rev. Nucl. Part. Sci. **44**, 27 (1994).
[18] M. B. Tsang *et al.*, Phys. Rev. C **53**, R1057 (1996).
[19] M. B. Tsang *et al.*, Phys. Rev. Lett. **78**, 3836 (1997).
[20] M. Huang *et al.*, Phys. Rev. Lett. **78**, 1648 (1997).
[21] M. D'Agostino *et al.*, Phys. Rev. Lett. **75**, 4373 (1995).
[22] M. D'Agostino *et al.*, Phys. Lett. B **368**, 259 (1996); M. D'Agostino *et al.*, in *XXXV International Winter Meeting on Nuclear Physics*, Bormio, 1997, edited by I. Iori (Ricerez Scientificz ed Educazione Permanente, Milano, 1997), p. 276.
[23] M. D'Agostino *et al.*, Phys. Lett. B **371**, 175 (1996).
[24] A. S. Botvina *et al.*, Nucl. Phys. **A475**, 663 (1987); J. P. Bondorf *et al.*, Phys. Rep. **257**, 133 (1995).
[25] W. Bauer, Phys. Rev. C **51**, 803 (1995).
[26] H. Xi *et al.*, Phys. Rev. C **57**, R462 (1998).
[27] H. Xi *et al.*, NSCL-MSU report 1055, 1997.
[28] P. F. Mastinu *et al.*, Phys. Rev. C **57**, 831 (1998).
[29] S. K. Samaddar *et al.*, Phys. Rev. Lett. **77**, 4962 (1997).
[30] C. B. Das and L. Satpathy, Phys. Rev. C **57**, R35 (1998).
[31] D. Cussol *et al.*, Nucl. Phys. **A561**, 298 (1993).
[32] J. Peter *et al.*, Nucl. Phys. **A593**, 95 (1995).
[33] M. Belkacem *et al.*, Phys. Rev. C **54**, 2435 (1996).